Automatic reverse turn of agricultural vehicles: a predictive approach

Christophe Cariou*, Roland Lenain*, Benoit Thuilot[†], Philippe Martinet[†]

* Cemagref	[†] LASMEA
24, av. des Landais	24, av. des Landais
63172 Aubière Cedex France	63177 Aubière Cedex France
christophe.cariou@cemagref.fr	benoit.thuilot@lasmea.univ-bpclermont.fr

Abstract— This paper addresses the automation of farm vehicle manoeuvres in headlands. A trajectory generation strategy is presented to plan reverse turns. Then, both steering and speed control algorithms are presented to guide the vehicle on the planned path, based on its kinematic model extended with additional sliding parameters and on predictive approaches. Real world experiments have been carried out on a low adherent terrain with an experimental mobile robot. At the end of each row, the sequences of the reverse turn are automatically generated to connect the next track to be followed, and the manoeuvre is autonomously performed by the vehicle. Reported experimental results demonstrate the capabilities of the proposed algorithms in full scale conditions.

I. INTRODUCTION

With a world population exceeding 6 billion and growing by about 6 million a month, the need to increase agricultural production while reducing the negative impacts of farm activity on the environment has become critical. Although modern agriculture allowed to double the world food production in 35 years, intensive use of inputs (chemical fertilizers, pesticides, herbicides) and increasingly size of farm vehicles are currently questioned due to their major degrading effects on the aquatic and terrestrial ecosystems. Therefore, new solutions are today required to develop environmentally sustainable agricultural productions. In this framework, as pointed out in [3] and [7], precision agriculture together with the development of automatic guided vehicles constitutes a promising way in terms of accuracy, repeatability, durability and field efficiency.

Numerous auto-steering systems have already been proposed and marketed for semi-autonomous tractors to accurately follow parallel tracks in the field (*e.g. Agco autoguide, Agrocom e-drive, Autofarm autosteer, John-Deere autotrac, Trimble aggps, Reichhardt autosteer*). However, the driver has still to manually turn the vehicle at the end of each row. In order to benefit of fully automated solutions, the automation of manoeuvres in headlands is required. Very few approaches have been proposed in that way, moreover mainly based on loop turns (*e.g. John-Deere itecpro*), [12]. The drawback of such an approach is that it involves excessive headland width for turning on the adjacent track, and is thereby far from optimal in term of productivity, headland being usually low-yield field areas due to high soil compaction.

A more efficient solution is to perform reverse turns, i.e. manoeuvres executed with stop points and reverse motion, leading to reduced headlands, see figure 1. This type of manoeuvre is widely used by farmers and more in accordance with agricultural European practices.
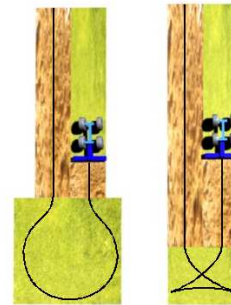

Fig. 1. Loop turn and reverse turn

However, automation of such reverse turns is a challenging problem in both path planning and control point of views, all the more that wheel skidding and slipping are inevitable in an agricultural context and may seriously damage the accuracy of path tracking as pointed out in [11]. Delays induced by steering and speed actuators may also lead to transient lateral overshoots when the vehicle enters into curves, or longitudinal overshoots when it stops.

In the litterature, most wheeled mobile robot controllers have been developed without sliding and actuators delays accounted. Moreover, numerous researches only focused on planning the global trajectories in the whole field to increase field efficiency [1], and seldom are the works related to manoeuvres generation in headlands [9].

This paper proposes to address this issue and is organized as follows. First, a trajectory generation strategy is presented based on clothoid arcs and primitives connected together to easily plan reverse turns. Then, the steering controller is considered, based as in our previous work on the control of two [5] and four [2] wheel steering vehicles on a kinematic model extended with additional sliding parameters to take into account for sliding phenomena. A predictive control algorithm is also used to reduce the effects induced by both steering actuation delays and agricultural machines inertia. Then, the velocity controller is designed based on a model predictive approach in order to anticipate for vehicle speed variations. Next, the experimental mobile robot is presented, and the capabilities of the proposed algorithms are finally insvestigated through full-scale experiments during reverse turns on a slippery ground.

II. REVERSE TURN PATH PLANNING

The planning of a reverse turn consists to generate three sucessive movements to connect two adjacent tracks AB and CD, separated of a distance $Dist$ as depicted figure 2. The trajectories should be admissible for the front two-wheel steering vehicle considered. The wheels must stay in the headland H whereas the body can go over as we suppose that none obstacle can touch the vehicle body.
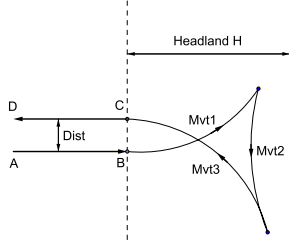

Fig. 2.   Three movements for reverse turn

The optimal trajectories are a compromise between the minimization of both the headland size and the time required to carry out the manoeuvres. Such problem is complex. Numerical algorithms are sometimes presented in the litterature [6] considering the problem as a minimum-time optimal control problem. Unfortunately, the minimization of the headland size is not addressed, and the developed algorithms generally demand high computational cost, leading to offline solutions and preliminary fixed trajectories. Online algorithms could nevertheless take advantage of the real-time measurements as the actual position and heading of the vehicle at the stop points to adapt the reverse turn online, optimising consequently the field coverage. In this paper, we propose to generate the manoeuvres using elementary primitives (line segment, arc of circle) connected together with clothoid arcs in order to ensure the curvature continuity of the motions. The obtained trajectories are certainly not optimal but could easily be adapted in real-time in future work, and enable to rapidly test the control algorithms.

A. Clothoid to connect a line segment and an arc of circle

The aim is to use an arc of clothoid to connect a line segment to an arc of circle. The curvature c of a clothoid varies linearly with respect to its curvilinear abscissa s, according to the constant g, see generic equation (1) and corresponding shape illustrated on figure 3(b). For the vehicle considered, g can be estimated using both the maximal angular velocity of the wheels $(20°/s)$ and the maximal vehicle linear velocity $(1m/s)$ during the reverse turn, i.e. a wheels rotation of $0.2°/cm$. Using the geometric relationship (2) supplying the front wheel steering vehicle curvature with respect to the front steering angle δ_F and the vehicle wheelbase $L = 1.2m$, it can be estimated that for a wheels rotation of $d\delta_F = 0.2°$ corresponds a curvature variation $dc = \frac{tan(d\delta_F)}{L} = 0.0029$, i.e. $g = \frac{dc}{ds} = 0.29$ with $ds = 0.01m$. Obviously, on one hand, this calculation depends of the wheels rotation angle, the vehicle curvature variation being greater for the same

$d\delta_F$ at high wheel angles as depicted on figure 3(a), and on the other hand, only a portion of the clothoid presented on figure 3(b) can be performed by the vehicle until the curvature corresponding to the minimum radius of curvature for the considered vehicle.

$$c(s) = g.s \qquad (1)$$

$$c = \frac{tan\delta_F}{L} \qquad (2)$$
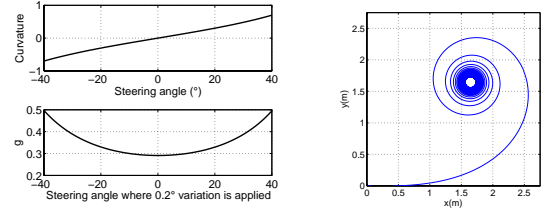
(a) Estimation of g   (b) Clothoid, $g = 0.29$

Fig. 3.   Estimation of g and clothoid

As expressed in [10] for highway design, the Cartesian coordinates of the clothoid $(x(s), y(s))$ can be written using the Fresnel integrals (3), which can be approximated using different methods, e.g. development in Taylor series.

$$\begin{cases} x(s) = \sqrt{\frac{\pi}{g}} \int_0^{\sqrt{\frac{g}{\pi}}s} \cos\left(\frac{\pi}{2}t^2\right) dt \\ y(s) = \sqrt{\frac{\pi}{g}} \int_0^{\sqrt{\frac{g}{\pi}}s} \sin\left(\frac{\pi}{2}t^2\right) dt \end{cases} \qquad (3)$$

To connect a line segment AB to an arc of circle MN of curvature $1/r$, see figure 4, with r corresponding to the minimum curvature radius of the vehicle, the points of the clothoid $(x(s), y(s))$ are calculated with (3) until the abcissa $s_1 = 1/g.r$ is reached. The coordinates of the center I of the circle are then given by (4). The arc of clothoid BM is thus entirely defined, leading to a continuous curvature trajectory admissible for the vehicle.

$$\begin{cases} x_I = r[\sqrt{2\pi\theta_1}A(\sqrt{\frac{2\theta_1}{\pi}}) - \sin\theta_1] \\ y_I = r[\sqrt{2\pi\theta_1}B(\sqrt{\frac{2\theta_1}{\pi}}) + \cos\theta_1] \end{cases} \quad with \ \theta_1 = g\frac{s_1^2}{2} \quad (4)$$
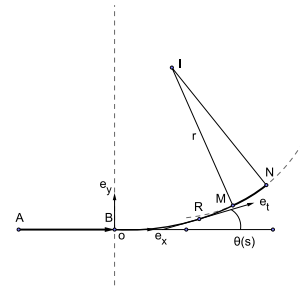

Fig. 4.   Connection with an arc of clothoid

B. Trajectory generation strategy

The proposed approach consists in the following steps.

- Firstly, the third movement from R to C is calculated, see figure 5, so that the vehicle at point R is parallel to the headland limit. On one hand, this specifies the size of the required headland to perform the reverse turn. On the other hand, it will enable to easily calculate the reverse turn for different values of the distance $Dist$, just adjusting the length of the line segment RT parallel to the headland limit.
- The first movement is calculated, composed of the arc of clothoid $Clo1$ and the circle of centre $I1$.
- Then, the second movement, i.e. the reverse movement, is built, composed of three arcs of clothoid and the third circle. $Clo4$ enables to go from curvature $c = 0$ at T to $c = c_{max}$ at X. $Clo3$ goes from curvature $c = c_{max}$ at X to $c = 0$ at Y, and $Clo2$ goes from $c = 0$ at Y to the circle curvature at Z.
- The second movement is vertically positionned in order to have an intersection point S between the first and third circle, that determines the position of the circle center $I3$. At the stop point S, the direction of the wheels will be reorientated to change the vehicle rotation instantaneous center from I to $I3$.
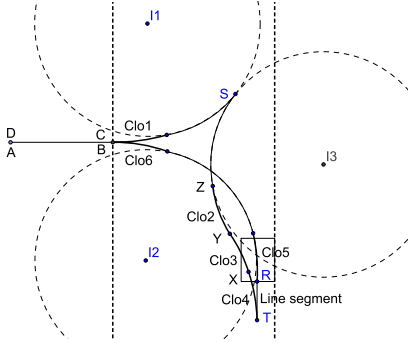

Fig. 5. Example with Dist=0

Figures 6(a) and 6(b) are respectively the results of the path planning algorithm for $Dist = 0$ and $Dist = 2m$.
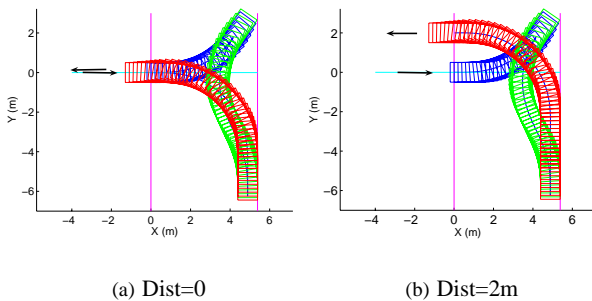

(a) Dist=0   (b) Dist=2m

Fig. 6. Reverse turn path planning

C. Speed references

We define the speed references with respect to the curvilinear abscissa for the three movements using sigmoid curves to limit the skidding at each beginning/end of movements. The maximal acceleration of the vehicle is about $1m/s^2$. The proposed sigmoid enables to go from 0 to $1m/s$ in $2m$ with a maximal acceleration of $0.65m/s^2$, see figure (7).
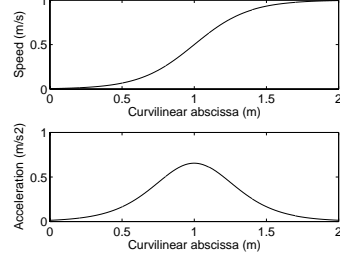

Fig. 7. Sigmoid as speed references

Thereby, at the end of each track, the trajectories of the reverse turns can now be automatically generated with linked speed references according to the chosen value $Dist$. The next section presents the control algorithms developed to accurately follow such reverse turns.

III. CONTROL ALGORITHMS

Accurate automatic guidance of mobile robots in an agricultural environment constitutes a challenging problem, mainly due to the low grip conditions usually met in such a context. As pointed out in [11], if the control algorithms are designed from pure rolling without sliding assumptions, the accuracy of path tracking may be seriously damaged, especially in curves. Therefore, sliding has to be accounted in the control design to preserve the accuracy of path tracking, whatever the path to be followed and soil conditions. Moreover, the actuations delays may lead to significant overshoots, especially at each beginning/end of curves and at each stop points. Predictive actions have then to be defined in order to maintain accurate path tracking performances.

Subsection A presents an extended kinematic model accounting for sliding effects and addresses the estimation of grip conditions using an observation algorithm. Subsection B describes the steering and speed control algorithms based on predictive approaches.

A. Kinematic model extended with sliding parameters

In the same way than in our previous work [5], two parameters homogeneous with side slip angles in a dynamic model are introduced to extend the classical two-wheel steering kinematic model, see the bicycle representation of the vehicle on figure 8. These two angles denoted respectively β_F and β_R for the front and rear axle represent the difference between the theoretical direction of the linear velocity vector at wheel centers, described by the wheel plane, and their actual direction. These angles are assumed to be entirely representative of the sliding influence on vehicle dynamics.

The notations used in this paper are listed below and depicted on figure 8.

- F and R are respectively the center of the front and rear virtual wheels. R is the point to be controlled.
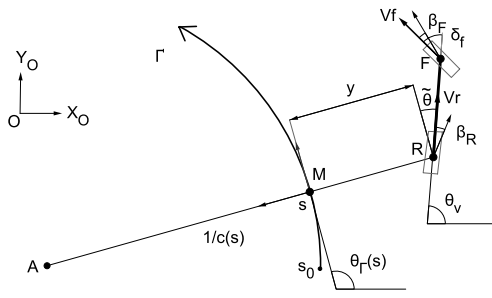
Fig. 8.   Path tracking parameters

Fig. 9.   Observer principle scheme

- θ_v is the orientation of vehicle centerline with respect to an absolute frame $[O, X_O, Y_O]$.
- δ_F is the front steering angle and constitutes the first control variable.
- V_r is the vehicle linear velocity at point R and constitutes the second control variable.
- β_F and β_R are the front and rear side slip angles.
- M is the point on the reference path Γ to be followed, which is the closest to R.
- s is the curvilinear abscissa of point M along Γ.
- $c(s)$ is the curvature of the path Γ at point M.
- $\theta_\Gamma(s)$ is the orientation of the tangent to Γ at point M with respect to the absolute frame $[O, X_O, Y_O]$.
- $\tilde{\theta} = \theta_v - \theta_\Gamma$ is the vehicle angular deviation.
- y is the vehicle lateral deviation at point R.
- L is the vehicle wheelbase (line segment RF).

The equations of motion are derived with respect to the path Γ. It can be established (see [5]) that:

$$\begin{cases} \dot{s} & = & V_r \frac{\cos(\tilde{\theta}-\beta_R)}{1-c(s)\,y} \\ \dot{y} & = & V_r \sin(\tilde{\theta} - \beta_R) \\ \dot{\tilde{\theta}} & = & V_r \left[\cos(\beta_R)\lambda_1 - \lambda_2\right] \end{cases} \quad (5)$$

with: $\lambda_1 = \frac{\tan(\delta_F - \beta_F)+\tan(\beta_R)}{L}$, $\lambda_2 = \frac{c(s)\cos(\tilde{\theta}-\beta_R)}{1-c(s)\,y}$

Model (5) accurately describes the vehicle motion in presence of sliding as soon as the two additional parameters β_F and β_R are known. We developed an observation algorithm to achieve side slip angles indirect estimation, relying on the sole lateral and angular deviations measurements, see [4]. This observer is based on the duality between observation and control, and is studied as a classical control problem. The principle scheme of this observer is presented figure 9. β_F and β_R are considered as control variables to be designed in order to ensure the convergence of the extended model outputs $(y, \tilde{\theta})_{obs}$, to the measured variables $(y, \tilde{\theta})_{mes}$.

B. Control laws design

The extended model (5) constitutes a relevant basis for mobile robot control design. The control objective is on one hand to perform a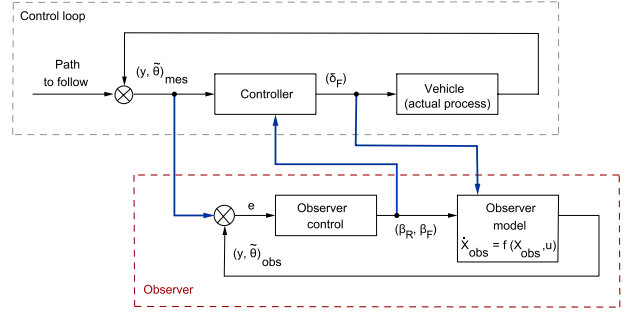n accurate path tracking with respect to lateral and angular deviations, and on the other hand to control the vehicle velocity on the planned speed references.

1) Steering controller: Our previous work [5] turns (5) into chained form and derived the steering control law for the front axle (6) where K_d is a gain allowing to specify a settling distance.

$$\begin{aligned} \delta_F & = & \beta_F + \arctan\Big\{\tan(-\beta_R) \\ & & + \frac{L}{\cos(\beta_R)}\big(\frac{c(s)\cos\tilde{\theta}_2}{\alpha} + \frac{A\cos^3\tilde{\theta}_2}{\alpha^2}\big)\Big\} \end{aligned} \quad (6)$$

with:

$$\begin{cases} \tilde{\theta}_2 & = & \tilde{\theta} - \beta_R \\ \alpha & = & 1 - c(s)y \\ A & = & -\frac{K_d^2 y}{4} - K_d\,\alpha\tan\tilde{\theta}_2 + c(s)\alpha\tan^2\tilde{\theta}_2 \end{cases} \quad (7)$$

To reject transient overshoots in lateral deviation when the vehicle enters into a curve mainly due to delays induced by the steering actuator, a predictive algorithm was also designed, see [4]. Experimental results demonstrated that high accurate guidance can be achieved whatever the grip conditions and the shape of the path to be followed.

However, the vehicle velocity was manually controlled and strictly positive. The idea in this paper is to extend these results and take advantage that the path following performances were demonstrated to be independent from the vehicle velocity, in order to built a second control loop dedicated for the vehicle speed control and therefore enable to autonomously perform the reverse turns.

2) Speed controller: Usually, when a vehicle stops at a point, signifiant overshoots in longitudinal motion is usually observed, mainly due to engine delay and vehicle inertia if not accounted in the controller. One way to reject such problem, and anticipate speed variations, is to design a predictive algorithm. To achieve this objective, the technique of model predictive control, based on theory developed in [8], is used.

Since the shape of the reference path and speed references are totally known, the desired value D for the velocity after an horizon of prediction H is inferred from current vehicle velocity $V(n)$ at time nT_e, see figure 10.

The approach consists to calculate the value of the control variable $C(n)$ to be sent to the speed actuator, which
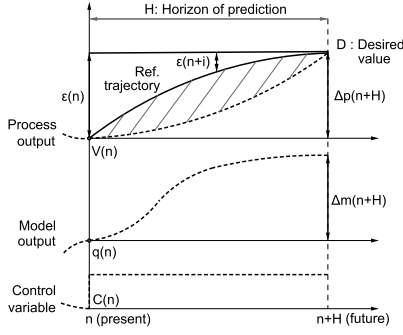
Fig. 10.   Model predictive control

will minimize the difference between a reference trajectory tending towards D and the prediction of the evolution of the velocity V during the horizon of predition H.

The reference trajectory is chosen with a first order dynamic (8), with $\epsilon(n) = D - V(n)$ and $\lambda = 0.6$ the decrement. The required increment Δp at time $n+H$ is (9). The required increment of the model is (10).

$$\epsilon(n+i) = \epsilon(n)\lambda^i \qquad (8)$$

$$\Delta p(n+H) = \epsilon(n) - \epsilon(n+H) = [D - V(n)](1 - \lambda^H) \quad (9)$$

$$\Delta m(n+H) = \Delta p(n+H) = q(n+H) - q(n) \qquad (10)$$

Considering the control variable $C(n)$ as a simple step and the vehicle longitudinal behavior as a first order of time constant $\tau = 0.42s$ and gain $K = 0.97$, see figure 11 and model equation (11), the speed control is then given by (12).

$$q(n+H) = q(n)e^{\frac{-H}{\tau}} + C(n)K(1 - e^{\frac{-H}{\tau}}) \qquad (11)$$

$$C(n) = \frac{[D - V(n)](1 - \lambda^H) + q(n) - q(n)e^{\frac{-H}{\tau}}}{K(1 - e^{\frac{-H}{\tau}})} \qquad (12)$$
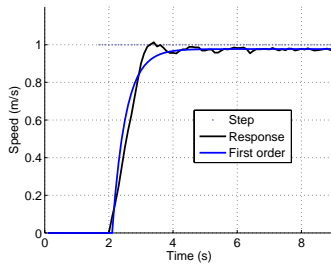

Fig. 11.   Longitudinal step response: identification with 1st order

IV. EXPERIMENTAL RESULTS

In this section, capabilities of the proposed control algorithms are investigated on the front two-wheel steering experimental mobile robot depicted on figure 12. Path planning and following of a reverse turn are tested on a natural terrain composed of irregular and wet grass. The vehicle weight and maximum speed are respectively $600kg$ and $18km/h$.

The only exteroceptive sensor on-boarded is an RTK-GPS receiver, whose antenna has been located straight up the center of the vehicle rear axle. It supplies an absolute position accurate to within 2cm, at a 10Hz sampling frequency.

Fig. 12.   Experimental platform

In our first experiments, the vehicle heading was derived from velocity vectors measurement from GPS. However, the main drawback of such an approach is that the heading accuracy strongly depends on the vehicle velocity. In fact, at very low speed, even after being processed through a Kalman state reconstructor, the obtained heading was very noisy and disturbed closed-loop vehicle behaviour. Therefore, a gyrometer was also embedded in the vehicle to obtain an accurate heading of the vehicle during the manoeuvres at low speeds.

In the forthcoming experimental tests, the track AB is firstly recorded during a preliminary run achieved in manual driving. The reverse turn at the end of the track is automatically calculated with $Dist = 2m$, as well as the trajectory back CD. Then, the path is autonomously followed by the vehicle using (6) and (12) control laws, see figure 13.
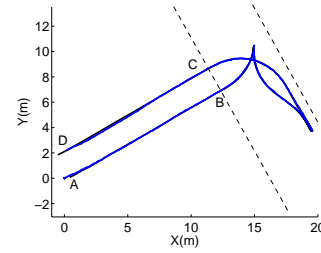

Fig. 13.   Results of the path following

As it can be seen on figures 14(a), the speed reference is correctly followed by the vehicle. The speed variations are well anticipated with the predictive approach. Figure 15 reports the measured and control signals of the front steering angle. We observe that the measured angle of the wheels follows correctly the steering control and reaches values of $\pm 20°$ with fast variations to perform the reverse turn.

The lateral deviation according to the curvilinear abscissa is reported on figure 16. In spite of fast speed and steering variations, an overall tracking error within $\pm 5cm$ is obtained, except at the end of the second stop point with a lateral error of $10cm$, certainly due to a too short horizon of prediction at this moment in the steering prediction algorithm together

with sliding conditions. The control gains (K_p, K_d) of (7) were set to $(0.19, 1.4)$ in order to impose a short settling distance $(6m)$ for the convergence of the lateral deviation. We can effectively noticed the obtained settling distance about $5m$ on figure 16.
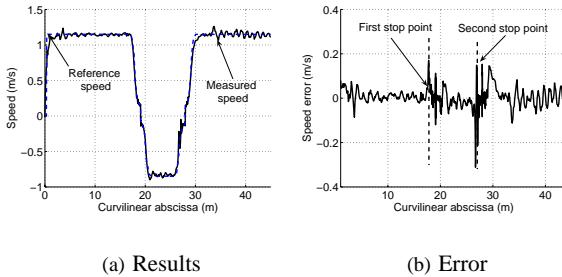

(a) Results   (b) Error
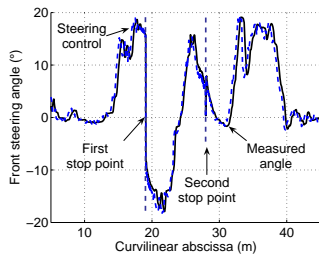
Fig. 14. Speed control
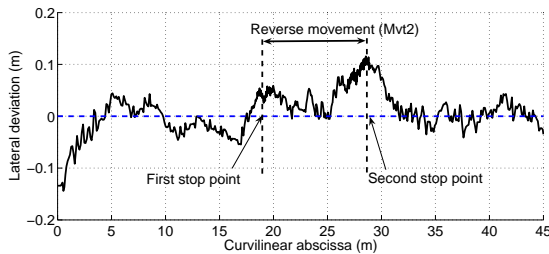

Fig. 15. Steering control

Fig. 16. Lateral deviation

Therefore, these experimental tests show the capability of the proposed approach to control an off-road vehicle on a planned reverse turn.

V. CONCLUSIONS AND FUTURE WORK

This paper adresses the problem of the automation of farm vehicles manoeuvres in headlands.

A reverse turn path planning algorithm is fisrtly presented. The trajectories are built using elementary primitives (line segment, arc of circle) connected together with clothoid arcs in order to ensure the curvature continuity of the movements. The simple trajectory generation strategy permits to easily adapt the reverse turn in real-time to connect adjacent tracks, and constitutes a suitable basis for testing the path tracking control algorithms.

An extended kinematic model accounting for sliding effects via two additional side slip angles is then presented.

This model is used to derive a steering control algorithm independent from the vehicle velocity. A second control loop dedicated for the vehicle speed control is then investigated in this paper, based on a model predictive control to anticipate the speed variations and compensate for vehicle inertia and low-level capabilities.

Promising results are presented with an experimental mobile robot on a natural environment. In spite of fast speed and steering variations required to perform the manoeuvres, an overall tracking error within $\pm 5cm$ is obtained, except at the second stop point around $10cm$. Such results are satisfaying in agricultural point of view. In fact, the aim in that case is not to obtain an accurate feedback stabilization on the stop points, difficult to perform all the more in sliding conditions, but to reach a bounded configuration around the stop point to enable reverse turn enough accurate for agricultural vehicles.

The follow-up of this work concerns the increase in the speed references to test the behaviour of the closed-loop system around the maximal acceleration of the vehicle requiring the development a skidding observer. The extension of such reverse turn with a four-wheel steering vehicle is also currently studied to explicitly control both lateral and angular deviations, see first developments on path following in [2]. Moreover, the case of the reverse turn with a trailer hooked to the vehicle will be also investigated. Since we are concerned with agricultural applications, the reverse turn of large trailers constitutes another challenging problem, all the more in sliding and skidding conditions.

REFERENCES

[1] Bochtis D.D., Vougioukas S.G. *Minimising the non-working distance travelled by machines operating in a headland field pattern* Biosystems engineering 101:1-12, 2008.

[2] Cariou C., Lenain R., Thuilot B., Martinet P. *Adaptive control of four wheel steering off road mobile robots: application to path tracking and heading control in presence of sliding* IEEE/RSJ Int. conf. on intelligent robots and systems, Nice, France, September 22-26, 2008.

[3] Katupitiya J., Eaton R., Yaqub T. *Systems engineering approach to agricultural automation: new developments* In IEEE Systems Conference, Honolulu, Hawai, USA April 9-12 2007.

[4] Lenain R., Thuilot B., Cariou C., Martinet P. *Adaptive and predictive path tracking control for off-road mobile robots* European journal of control, 13(4):419-439, 2007.

[5] Lenain R., Thuilot B., Cariou C., Martinet P. *High accuracy path tracking for vehicles in presence of sliding. Application to farm vehicle automatic guidance for agricultural tasks* Autonomous robots, 21(1):79-97, 2006.

[6] Oksanen T. *Path planning algorithms for agricultural field machines* Helsinki university of technology, research reports No 31, 2007.

[7] Pedersen S.M., Fountas S., Have H., Blackmore B.S. *Agricultural robots - system analysis and economic feasibility* Precision Agriculture, 7(4):295-308, 2006.

[8] Richalet J.. *Industrial applications of model based predictive control* Automatica, 29:1251-1574, 1993.

[9] Vougioukas S., Blackmore S., Nielsen J., Fountas S. *A two-stage optimal motion planner for autonomous agricultural vehicles.* Precision Agriculture, 7:361-377, 2006.

[10] Walton D.J. *Spiral spline curves for highway design.* Microcomputers in civil engineering 4:99-106, 1989.

[11] Wang D., Low C. B. *Modeling skidding and slipping in wheeled mobile robots: control design perspective.* In Proc. of the IEEE int. conf. on Intelligent Robots and Systems, Beijing, China, Oct 2006.

[12] Zhu Z., Chen J., Yoshida T., Torisu R., Song Z., Mao E. *Path tracking control of autonomous agricultural mobile robots.* Journal of Zhejang University Science A 8(10):1596-1603, 2007.